Electronic Supplementary Information for Dalton Transactions

Supplementary Information

Unique assembly of low-dimensional viologen iodoplumbates and their improved semiconducting properties

Yang Chen,[ab] Zi-Ou Wang,[c] Zhou Yang,[a] Zhi-Gang Ren,[a] Hong-Xi Li,[a] and Jian-Ping Lang[*ab]

[a]*College of Chemistry, Chemical Engineering and Materials Science, Suzhou University, Suzhou 215123, Jiangsu, P. R. China*

[b]*State Key Laboratory of Organometallic Chemistry, Shanghai Institute of Organic Chemistry, Chinese Academy of Sciences, Shanghai 200032, P. R. China*

[c]*College of Electronics and Information Engineering, Suzhou University, 1 ShiZi Street, Suzhou 215006, Jiangsu, P. R. China*

Table of Contents

Experimental Section

General procedures. All chemicals and reagents were obtained from commercial sources and used as received. The elemental analyses for C, H and N were performed on a Carlo–Erba CHNO–S microanalyzer. The IR spectra were recorded on a Varian 1000 FT–IR spectrometer as KBr disks (4000-400 cm^{-1}). ^1H NMR spectra were recorded at ambient temperature on a Varian UNITYplus-400 spectrometer. ^1H NMR chemical shifts were referenced to the solvent signal in d_6-DMSO. PXRD were performed using a PANalytical X'Pert PRO MPD system (PW3040/60).

Syntheses of $(Pb_{13}I_{38})(B'V)_6$ (**1**) and $[(Pb_5I_{14})(BV)_2]_n$ (**2**): To a Pyrex glass tube (15 cm in length, 7 mm in inner diameter) was added PbI_2 (23 mg, 0.05 mmol), iodine (13 mg, 0.05 mmol), 4,4'-bipy (8 mg, 0.05 mmol), benzyl alcohol (0.5 mL), water (3.0 μL) and acetonitrile (1.5 mL). The tube was sealed and heated in an oven at 150 °C for 35 h and then cooled to room temperature at a rate of 5 °C/100 min to form red cube crystals of **1** and red rod crystals of **2**, which were collected manually under microscope, washed with ethyl acetate, and dried in air. Yield for **1**: 13 mg (34 % based on PbI_2). Anal. Calcd for $C_{186}H_{168}N_{12}Pb_{13}I_{38}$: C, 22.15; H, 1.68; N, 1.67 %. Found: C, 22.47; H, 1.68; N, 1.55 %. IR (KBr, cm^{-1}): 3036m, 2931w, 1631s, 1552m, 1523w, 1494m, 1454s, 1423m, 1385m, 1353w, 1341w, 1278w, 1207w, 1187w, 1157m, 1078w, 1028w, 1002w, 971w, 923w, 895w, 839w, 810m, 764w, 737s, 697s, 651w, 624m, 597w, 555w, 517w, 463w. ^1H NMR (300 MHz, d_6-DMSO, 298 K, TMS): δ = 4.63 (s, 2H, $–CH_2–$), 5.94 (d, 4H, $–CH_2–$), 7.35 (m, 15H, Ph–H), 8.62 (m, 4H, Py–H), 9.27 (d, 1H, Py–H), 9.44 (d, 2H, Py–H). Yield for **2**: 11 mg (30 % based on PbI_2). Anal. Calcd for $C_{48}H_{44}N_4Pb_5I_{14}$: C, 16.52; H, 1.27; N, 1.61 %. Found: C, 16.44; H, 1.25; N, 1.53 %. IR (KBr, cm^{-1}): 3106w, 3089w, 3040m, 2955w, 2930w, 1632s, 1554m, 1494m, 1440s, 1384w, 1343m, 1277w, 1208m, 1157m, 1027w, 964w, 838w, 803m, 742m, 698m, 626w, 593w, 557w, 502w, 453w. ^1H NMR (300 MHz, d_6-DMSO, 298 K, TMS): δ = 5.94 (s, 4H, $–CH_2–$), 7.54 (q, 10H, Ph–H), 8.74 (d, 4H, Py–H), 9.51 (d, 4H, Py–H). Pure **2** could also be prepared as above using 0.5 mL water and 1.0 mL MeCN. Yield: 17 mg (47 % based on PbI_2).

Preparation of **2a**: To 0.1 M $ZnCl_2$ aqueous solution (8.0 mL) was added crystals of **2** (80 mg,

0.023 mmol). The mixture was sealed and kept it at room temperature for two weeks. The resulting crystals (**2a**) was washed with a large amount of deionized water ten times and dried in air.

Preparation of **2b**: To a Pyrex glass tube (15 cm in length, 7 mm in inner diameter) was added crystals of **2** (20 mg, 0.006 mmol) and 0.1 M $ZnCl_2$ aqueous solution (2.0 mL). The tube was sealed and heated in an oven at 80 °C for 12 h and then cooled to room temperature directly. The resulting crystals (**2b**) was washed with a large amount of deionized water ten times and dried in air.

X-ray diffraction crystallography: X-ray single-crystal diffraction data for **1** and **2** were collected on a Rigaku Mercury CCD diffractometer by using graphite monochromated Mo-Kα (λ = 0.71073 Å). Cell parameters were refined by using the program *CrystalClear* (Rigaku and MSC, version 1.3, 2001). The collected data were reduced by using the program *CrystalClear*, and an absorption correction (multiscan) was applied. The reflection data were also corrected for Lorentz and polarization effects. The crystal structures of **1** and **2** were solved by direct methods and refined on F^2 by full-matrix least-squares methods with the *SHELXL-97* program.[1] For **1**, one benzyl group in $B'V^{2+}$ was disordered over two positions, which were isotropically refined with an occupancy factor of 0.50/0.50 for C19~C24/C19'~C24'. All non-hydrogen atoms were refined anisotropically. All H atoms were introduced at the calculated positions and included in the structure-factor calculations. All the calculations were performed on a Dell workstation using the *CrystalStructure* crystallographic software package (Rigaku and MSC, Ver.3.60, 2004).

1 G. M. Sheldrick, *SHELXS-97and SHELXL-97. Program for the refinement of crystal structures*, University of Göttingen, Germany, 1997.

Table S1. Selected bond lengths (Å) and angles (°) for **1** and **2**

	Complex **1**		
Pb(1)-I(1)	3.2250(8)	Pb(2)-I(1)	3.3420(9)
Pb(2)-I(2)	3.1030(10)	Pb(2)-I(3)	3.0230(10)
Pb(2)-I(4)	3.1482(10)	Pb(2)-I(1A)	3.4295(9)
Pb(2)-I(7)	3.450(10)	Pb(3)-I(2)	3.2292(10)
Pb(3)-I(4A)	3.492(12)	Pb(3)-I(5)	2.9874(12)
Pb(3)-I(6)	3.1371(11)	Pb(3)-I(6A)	3.2471(11)
Pb(3)-I(7)	3.517(12)		
I(1)-Pb(1)-I(1A)	90.29(2)	I(2)-Pb(2)-I(3)	88.63(3)
I(3)-Pb(2)-I(4)	94.15(3)	I(2)-Pb(2)-I(4)	93.39(3)
I(1)-Pb(2)-I(3)	96.98(3)	I(1)-Pb(2)-I(2)	172.62(3)
I(1)-Pb(2)-I(4)	90.99(2)	I(3)-Pb(2)-I(1A)	91.66(2)
I(2)-Pb(2)-I(1A)	90.13(2)	I(4)-Pb(2)-I(1A)	173.27(3)
I(1)-Pb(2)-I(1A)	84.94(3)	I(3)-Pb(2)-I(7)	175.01(3)
I(7)-Pb(2)-I(1A)	85.59(3)	I(1)-Pb(2)-I(7)	86.93(3)
I(2)-Pb(2)-I(7)	87.22(3)	I(4)-Pb(2)-I(7)	88.85(3)
I(5)-Pb(3)-I(6)	92.97(4)	I(2)-Pb(3)-I(5)	88.32(4)
I(2)-Pb(3)-I(6)	94.32(3)	I(5)-Pb(3)-I(6A)	102.17(4)
I(6)-Pb(3)-I(6A)	90.20(4)	I(2)-Pb(3)-I(6A)	168.37(3)
I(2)-Pb(3)-I(4A)	86.31(4)	I(5)-Pb(3)-I(4A)	97.57(4)
I(4A)-Pb(3)-I(6A)	87.31(4)	I(6)-Pb(3)-I(4A)	169.45(4)
I(7)-Pb(3)-I(4A)	82.52(4)	I(2)-Pb(3)-I(7)	84.15(4)
I(5)-Pb(3)-I(7)	172.45(4)	I(7)-Pb(3)-I(6A)	85.38(4)
I(6)-Pb(3)-I(7)	87.07(4)		
	Complex **2**		
Pb(1)-I(1)	3.2288(11)	Pb(1)-I(2)	3.1770(12)
Pb(1)-I(3)	3.3154(11)	Pb(2)-I(1B)	3.2218(11)
Pb(2)-I(2A)	3.2285(11)	Pb(2)-I(3)	3.3635(11)

Pb(2)-I(3B)	3.4790(12)	Pb(2)-I(4)	3.1447(12)
Pb(2)-I(5)	3.0561(11)	Pb(3)-I(1A)	3.6130(13)
Pb(3)-I(3)	3.6780(13)	Pb(3)-I(4C)	3.2785(11)
Pb(3)-I(5)	3.1964(11)	Pb(3)-I(6)	2.9810(12)
Pb(3)-I(7)	3.0047(13)		
I(1)-Pb(1)-I(2)	86.31(3)	I(1)-Pb(1)-I(1A)	178.53(4)
I(1)-Pb(1)-I(2A)	92.65(3)	I(1)-Pb(1)-I(3)	86.61(3)
I(1)-Pb(1)-I(3A)	94.48(3)	I(2)-Pb(1)-I(2A)	90.95(4)
I(2)-Pb(1)-I(3)	172.30(2)	I(2)-Pb(1)-I(3A)	92.39(3)
I(3)-Pb(1)-I(3A)	85.16(4)	I(4)-Pb(2)-I(5)	86.20(4)
I(5)-Pb(2)-I(1B)	89.07(3)	I(4)-Pb(2)-I(1B)	94.69(3)
I(5)-Pb(2)-I(2A)	92.47(3)	I(4)-Pb(2)-I(2A)	87.00(3)
I(1B)-Pb(2)-I(2A)	177.79(3)	I(3)-Pb(2)-I(5)	85.81(3)
I(3)-Pb(2)-I(4)	171.55(3)	I(3)-Pb(2)-I(1B)	87.92(3)
I(3)-Pb(2)-I(2A)	90.60(3)	I(1B)-Pb2-I(3B)	84.02(4)
I(2A)-Pb2-I(3B)	94.39(4)	I(3)-Pb2-I(3B)	91.93(4)
I(4)-Pb2-I(3B)	96.32(4)	I(5)-Pb2-I(3B)	172.81(4)
I(3)-Pb(3)-I(1A)	82.45(4)	I(3)-Pb(3)-I(4C)	102.30(4)
I(3)-Pb(3)-I(5)	78.75(4)	I(3)-Pb(3)-I(6)	96.71(4)
I(3)-Pb(3)-I(7)	164.59(4)	I(5)-Pb(3)-I(6)	94.47(3)
I(5)-Pb(3)-I(7)	86.25(4)	I(5)-Pb(3)-I(1A)	99.25(4)
I(5)-Pb(3)-I(4C)	174.40(3)	I(6)-Pb(3)-I(1A)	175.96(4)
I(6)-Pb(3)-I(4C)	90.87(3)	I(6)-Pb(3)-I(7)	87.85(4)
I(7)-Pb(3)-I(1A)	93.98(4)	I(7)-Pb(3)-I(4C)	92.30(4)
I(1A)-Pb(3)-I(4C)	85.46(4)		

Symmetry codes: for **1**: A: $-x + y + 1, -x + 1$, z; for **2**: A: $-x, y, 1/2 - z$; B: $-x, 1 - y, 1 - z$; C: $x, 1 - y, z - 1/2$.

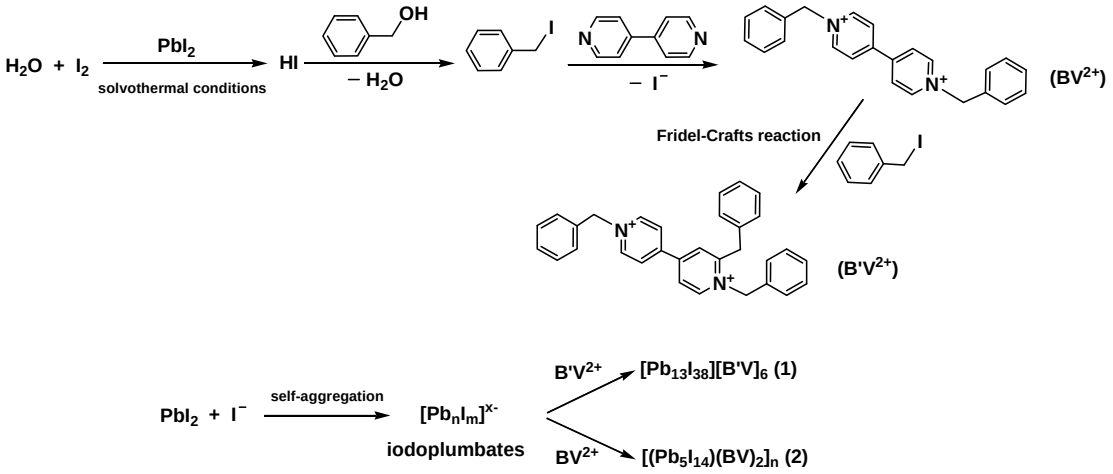

Scheme S1. The possible mechanisms for the formation of 1,1'-dibenzyl-4,4'-bipyridinium (BV^{2+}), 1,2,1'-tribenzyl-4,4'-bipyridinium ($B'V^{2+}$), and two low-dimensional viologen iodoplumbates ($[Pb_{13}I_{38}][B'V]_6$ (**1**), $[(Pb_5I_{14})(BV)_2]_n$ (**2**)) through solvothermal reactions of benzyl alcohol with 4,4'-bipy, PbI_2 and I_2 along with a trace amount of water in acetonitrile.

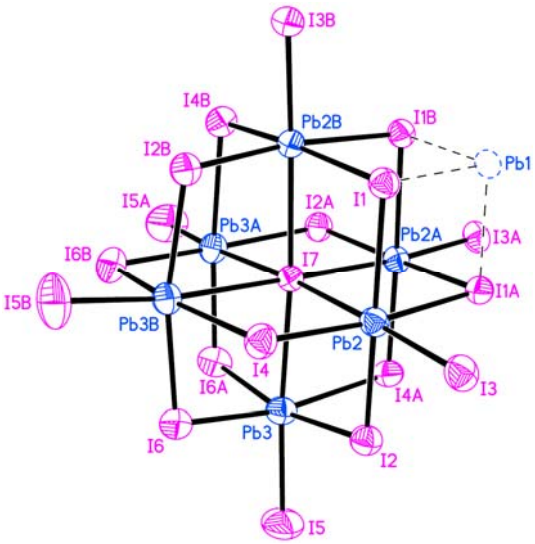

Figure S1. View of the $[Pb_6I_{19}]$ fragment in the $[Pb_{13}I_{38}]^{12-}$ anion of **1** with a labeling scheme and 50% thermal ellipsoids. Symmetry codes: A: $-x + y + 1, -x + 1, z$; B: $-y + 1, x - y, z$.

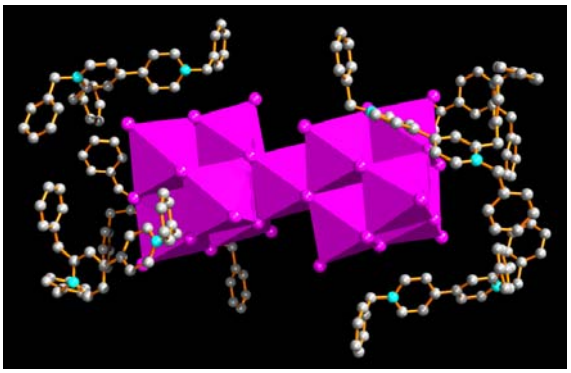

Figure S2. View of the $[Pb_{13}I_{38}]^{12-}$ anion in **1**. Each pink octahedron represents a PbI_6 unit. All H atoms have been omitted for clarity.

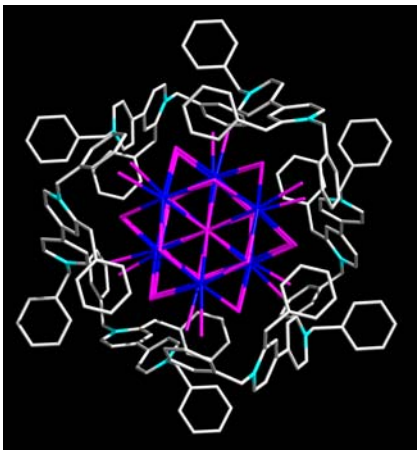

Figure S3. View of a Kagomé-like cavity of the molecular structure of **1** looking down along the *c*

axis. All H atoms have been omitted for clarity.

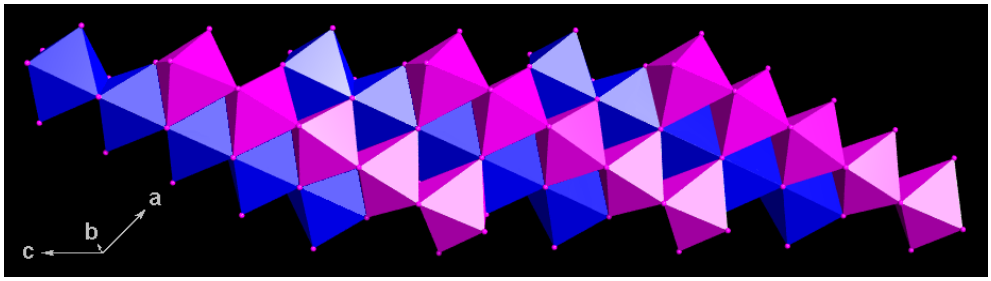

Figure S4. View of the double stranded iodoplumbate chain of **2**. Each octahedron represents a PbI_6 unit.

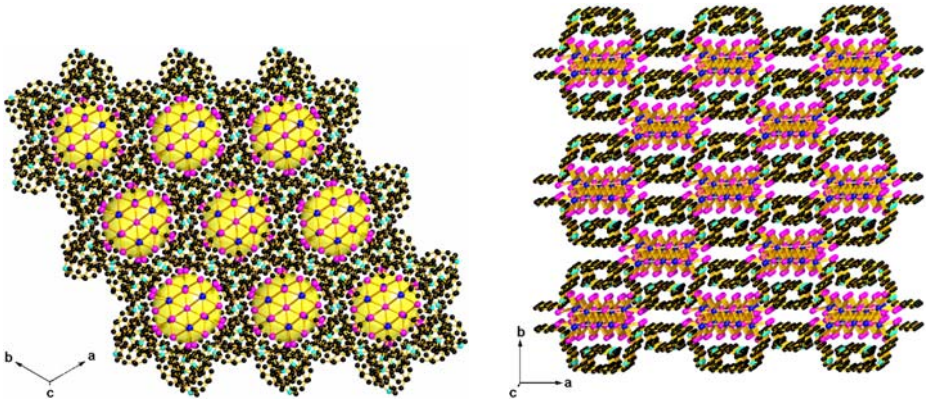

(a) **(b)**

Figure S5. Views of the 3D packing diagram of **1** (a) and **2** (b) looking down along the *c*-direction. Each yellow ball in (a) represents one $[Pb_{13}I_{38}]^{12-}$ anion in **1**. Atom color codes: C, black; N, cyan; Pb, blue; I, pink. All H atoms have been omitted for clarity.

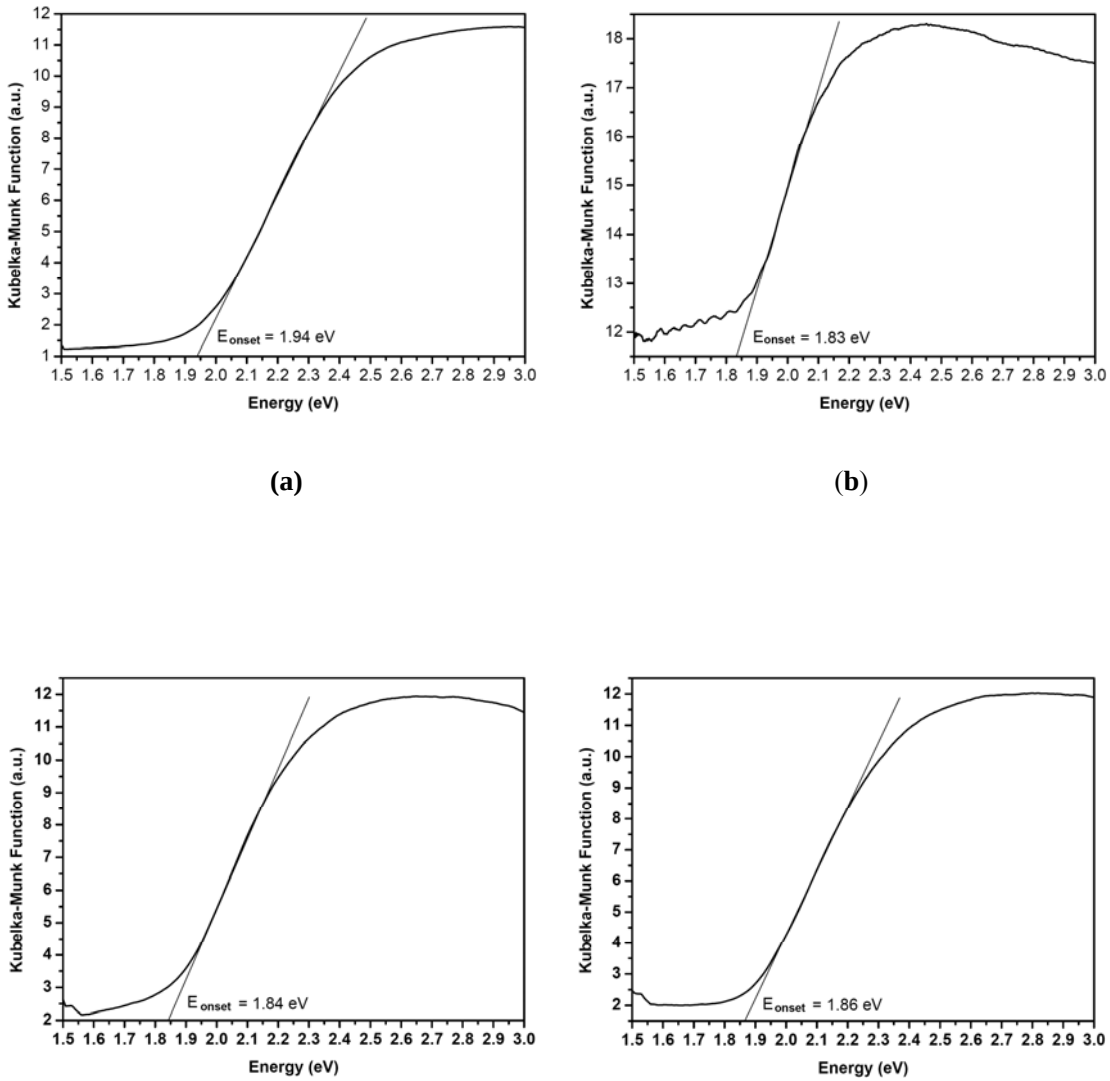

Figure S6. Solid-state optical diffuse-reflection spectra of **1** (a), **2** (b) along with two Zn/Cl-doped samples (**2a** (c), and **2b** (d)).

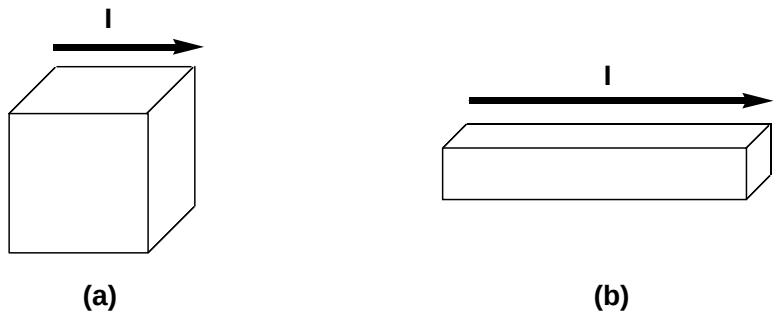

Figure S7. The flowing directions of current in single crystals of **1**(a), **2**(b) along with two Zn/Cl-doped samples (**2a**(b) and **2b**(b)). For the electric conductivity measurements, the conductive adhesive was used to fix the two ends of a single crystal, which were further connected with two conducting probes. This device was put on a thermostatic stage, and the conductivity along the fixed direction was measured by using an Agilent 4156C semiconductor parameter analyzer and Vector MX-1100B Prober. For each compound, five single crystals were selected out to measure. In the case of **1**, ten crystals were chosen because of the uncertainty of the direction for cube crystal. The final data were the average of the records.

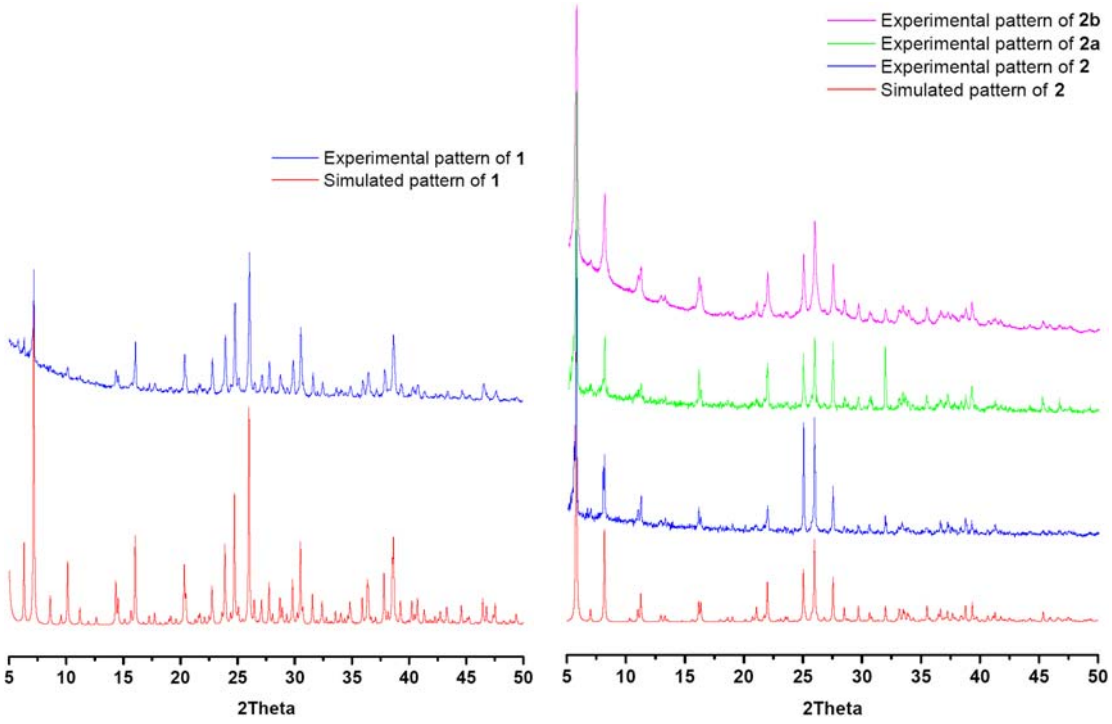

(**a**) (**b**)

Figure S8. Powder X-ray diffraction (PXRD) spectra of **1**, **2** along with two Zn/Cl-doped samples (**2a** and **2b**). (a) Experimental (blue line) and simulated (red line) patterns of **1**. (b) Experimental (blue line) and simulated (red line) patterns of **2** and experimental patterns of **2a** (pink line) and **2b** (green line).

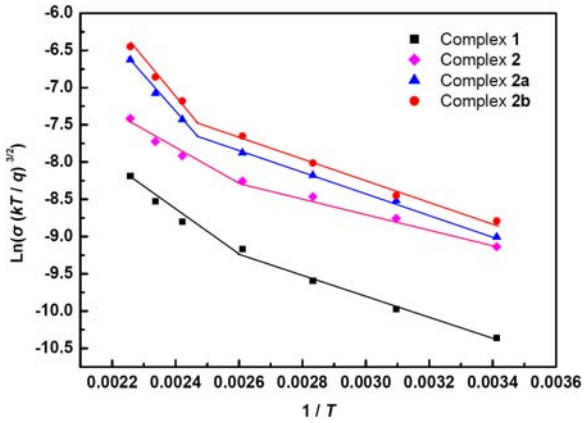

Figure S9. The plot of $1/T$ and $\mathrm{Ln}(\sigma(kT/q)^{3/2})$ based on Holstein model for **1**, **2**, **2a** and **2b**.